



# Dynamics of a camphoric acid boat at the air–water interface

V.S. Akella<sup>a,\*</sup>,<sup>1</sup>, Dhiraj K. Singh<sup>a</sup>, Shreyas Mandre<sup>b</sup>, M.M. Bandi<sup>a</sup>

<sup>a</sup> Collective Interactions Unit, OIST Graduate University, Okinawa 904-0495, Japan

<sup>b</sup> School of Engineering, Brown University, 182 Hope Street, Providence, RI 02906, USA

## ARTICLE INFO

### Article history:

Received 22 December 2017  
 Received in revised form 16 February 2018  
 Accepted 18 February 2018  
 Available online 21 February 2018  
 Communicated by Z. Siwy

### Keywords:

Marangoni propulsion  
 Self-motion

## ABSTRACT

We report experiments on an agarose gel tablet loaded with camphoric acid (c-boat) spontaneously set into motion by surface tension gradients on the water surface. We observe three distinct modes of c-boat motion: harmonic mode where the c-boat speed oscillates sinusoidally in time, a steady mode where the c-boat maintains constant speed, and an intermittent mode where the c-boat maintains near-zero speed between sudden jumps in speed. Whereas all three modes have been separately reported before in different systems, controlled release of Camphoric Acid (CA) from the agarose gel matrix allowed the observation of all the three modes in the same system. These three modes are a result of a competition between the driving (surface tension gradients) and drag forces acting on the c-boat. Moreover we suggest that there exist two time scales corresponding to spreading of CA and boat motion and the mismatch of these two time scales give rise to the three modes in boat motion. We reproduced all the modes of motion by varying the air–water interfacial tension using Sodium Dodecyl Sulfate (SDS).

© 2018 Elsevier B.V. All rights reserved.

## 1. Introduction

The self-motion is an essential part of biological life. In the animal kingdom, usually the chemical energy is converted into mechanical energy by various mechanisms. However, in the inanimate world, electrical or magnetic energy is converted into mechanical energy to drive the motion. In both the animate and inanimate worlds, a common mechanism for the self-motion is *via* the imbalance of surface tension known as *Marangoni propulsion*. These forces can be classified as solutal or thermal when a solute or temperature, respectively, modifies the surface tension. Tears-of-wine [1,2] is a classical example of solutal (or agent induced) Marangoni effect. Thermal Marangoni effects [3] are a commonly encountered phenomenon in welding industry.

The scientific interest in the motion of objects governed by the surface tension gradients started in 1686 with the first reported observations by Heyde [4]. Later, Alessandro Volta [5], Giovanni Battista Venturi [6], Biot [7] and Lord Rayleigh [8], among others, studied the motion of objects on the surface of water. However, Van der Mensbrugge [9] first explained that the motion is due to the modification of surface tension of water by the object. For

a historical introduction up until 1869 please see Charles Tomlinson's excellent review [10]. Since then many researchers have been studying motion of objects driven by the surface tension gradients. These studies are at Reynolds numbers spanning over 4–5 orders of magnitude ( $\sim 10^{-3}$ – $10^2$ ). Few examples are: motion of liquid droplets on a solid surface with surface energy gradient [11], motion of ethanol driven gel tablets on the air–water interface [12], propulsion of Belousov–Zhabotinsky drops in fluorinated oil [13], motion of camphor boats at the air–water interface [14], motion of solid/liquid composites on water [15]. Recently, Nagayama et al. [16] developed a simple mathematical model for self-propulsion driven by surface tension gradients. These systems continue to attract much attention due to the simplicity and robustness in preparation. Despite the rich history, the self-propelled particles/drops continue to remain relevant in modern times, be it in statistical mechanics within the context of active matter [17], hydrodynamic context of viscous Marangoni propulsion [18], biological context of chemo-mechanical transduction [19], autonomous motion and self-assembly [20], and reconfigurable actuators in soft matter physics [21], among others. More recently, Liang Hu et al. [22] successfully mimicked the motion of an amoeba-like motion by altering the surface properties of the liquid metal alloy.

In this article, we present an experimental study of the self-motion of agarose gel tablets loaded with camphoric acid (CA) at the air–water interface, henceforth referred to as c-boats. We identify three distinct modes of motion, namely a harmonic mode

\* Corresponding author.

E-mail address: sathishakella@gmail.com (V.S. Akella).

<sup>1</sup> Present address: Department of Applied Mechanics, IIT Madras, Chennai, Tamilnadu 600 036, India.

where the c-boat speed undergoes time-varying sinusoidal oscillations, a steady mode of constant c-boat motion, and an intermittent mode where the c-boat remains at rest between sudden jumps in speed and position at nearly regular time intervals. Whereas all three modes have been separately reported in the published record [23–25,12] in a variety of systems, we show these seemingly different self-propulsive modes arise from a common description. The camphoric acid boat system had been extensively studied by Nakata et al. [26,27] however control release of camphoric acid from the agarose gel matrix enabled us to observe all the three modes of oscillation in the same system. Through metered dosage of Sodium Dodecyl Sulfate (SDS) to control the air–water surface tension, we experimentally trace the origin of self-propulsive mode selection to CA–water surface tension difference.

## 2. Experimental methods

We constructed the camphoric acid boats (c-boats) by infusing camphoric acid in agarose gel tablets similar in spirit to the procedure of Soh et al. [28], thus keeping tablet structurally intact for the entire duration of the experiment. An important consequence of structural intactness is that the shape effects on drag are constant during the course of an experiment. Hot agarose solution (5% weight-to-volume) in de-ionized (DI) water (Milli-Q Integral Water Purification System with resistivity,  $\rho = 18.2 \text{ M}\Omega\text{-cm}$  at  $25^\circ\text{C}$ ) was placed between two clean glass plates, set  $10^{-3} \text{ m}$  apart with aluminum spacers, to obtain gel sheets of uniform  $10^{-3} \text{ m}$  thickness, upon cooling. Gel tablets of  $3 \times 10^{-3} \text{ m}$  diameter were punched out from the sheet (Biopunch, Ted Pella Inc.). These gel tablets were introduced in a saturated solution of camphoric acid (CA) (Wako Pure Chemical Industries, Ltd., Cat. No. 036-01002) in methanol and left for 2 hours for CA to diffuse into the gel tablets. Prior to experiments, gel tablets were rinsed in DI water to precipitate CA in the gel matrix.

Fig. 1a shows a schematic of the experimental setup. All experiments were performed in a glass petri dish (0.25 m in diameter) filled with de-ionized water to a height of 0.04 m. A c-boat was gently introduced at the air–water interface and its self-motion was recorded with a Nikon D800E camera at 30 frames per second. The petri dish was placed atop a uniform back-lit LED illumination source operating with direct current to avoid alternating current flicker interference in image processing. The c-boat appears as a dark disk moving against a bright background in the current imaging technique as shown in Fig. 1b. The experimental images were post-processed with image analysis algorithms written in-house to obtain the c-boat position and velocity as a function of time. The c-boat position and velocity information employed in the analysis was confined to a region 0.036 m away from the walls to exclude boundary effects. The portion of c-boat trajectory (red in Fig. 1b) lying outside the dashed white circle in Fig. 1b at a distance of 0.036 m from petri dish wall were excluded from the analysis. This 0.036 m exclusion distance was empirically determined from the longest radial distance over which Marangoni spreading of camphoric acid was prominent. Only blue sections of the c-boat trajectory within the inner circle bounded by white dashed line in Fig. 1b were used in all the analysis to follow. As mentioned earlier, a c-boat is driven by the surface tension gradients and to independently verify the role of surface tension on the three modes of c-boat motion, we varied the surface tension of the ambient interface by introducing metered dosage of Sodium Dodecyl Sulfate (SDS) (Wako Pure Chemical Industries, Ltd., Cat. No. 196-08675) following published tables [29]. Actual surface tension values were also independently confirmed with the pendant drop method on a tensiometer (OneAttention Theta tensiometer) at  $25^\circ\text{C}$ .

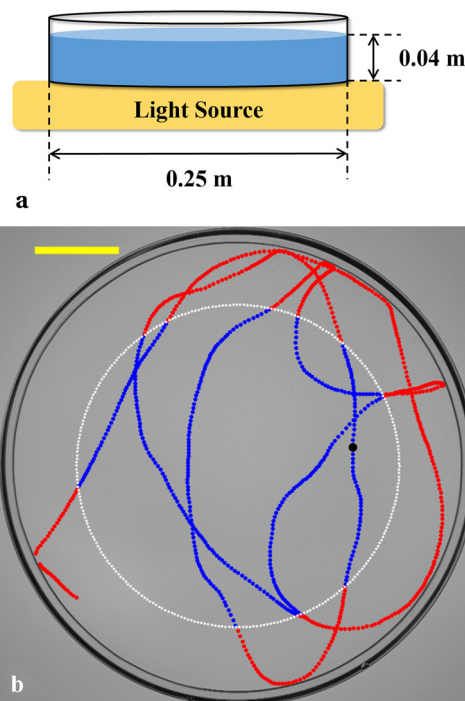


**Fig. 1.** (a) Experimental setup (side view): Glass petri dish (0.25 m diameter) filled with deionized water to 0.04 m height was placed on a light tablet. A camera recorded c-boat self-motion from above yielding images as shown in (b) where the c-boat appears as a dark disk in gray background. Only trajectories (blue) in a 0.178 m diameter circular region within the dashed white circle were analyzed and the rest (red) discarded to exclude boundary effects from petri dish wall. Scale bar = 0.03 m. (For interpretation of the colors in the figure(s), the reader is referred to the web version of this article.)

## 3. Results & discussion

Camphoric acid is a white crystalline organic compound and mildly soluble in water. When dissolved to the solubility limit ( $\sim 8 \times 10^{-3} \text{ kg}\cdot\text{l}^{-1}$ ), the surface tension of CA + Water solution is  $\sim 60 \text{ mN}\cdot\text{m}^{-1}$ . Soon after placing a c-boat on surface of water, there exists a thin annular region, immediately next to the boundary of the c-boat, where CA is adsorbed/dissolved and beyond the region the concentration of CA is zero. The surface tension is low in the annular region and is equal to the ambient surface tension ( $\gamma = 72 \times 10^{-3} \text{ N}\cdot\text{m}^{-1}$ ) outside. This results in sharp gradient/shock in surface tension which relaxes by spreading CA onto the surface (see movie *S1.avi* in supplementary info). This relaxation process gives rise to a time scale  $\tau_1$ , which will be discussed later. However, the spreading cannot continue indefinitely due to the dissolution of CA in water. On a side note, the CA spread radius scales with time as  $t^{1/2}$  (Fig. 2b). This is an experimentally well established [30] scaling for volatile oils spreading on water surface. Therefore, one can conclude that the scaling is identical when either evaporation/dissolution or both result in loss of material from the surface.

In the steady state, CA radially spreads to a finite distance  $R$  beyond which CA concentration is nearly zero and axially symmetric CA concentration gradients (and hence surface tension gradients) are set up around the c-boat. By virtue of the symmetric surface tension gradients there is *no* driving force on the boat but steady state Marangoni flows are generated in the underlying fluid. Ambient fluctuations spontaneously break this symmetry and sharpen the gradients along a preferential direction; as a consequence a net force acts on the c-boat and propels it (see *S2.avi* in the supplementary info). The c-boat motion enhances the asymmetry and the boat accelerates until (1) c-boat escapes to a CA free region

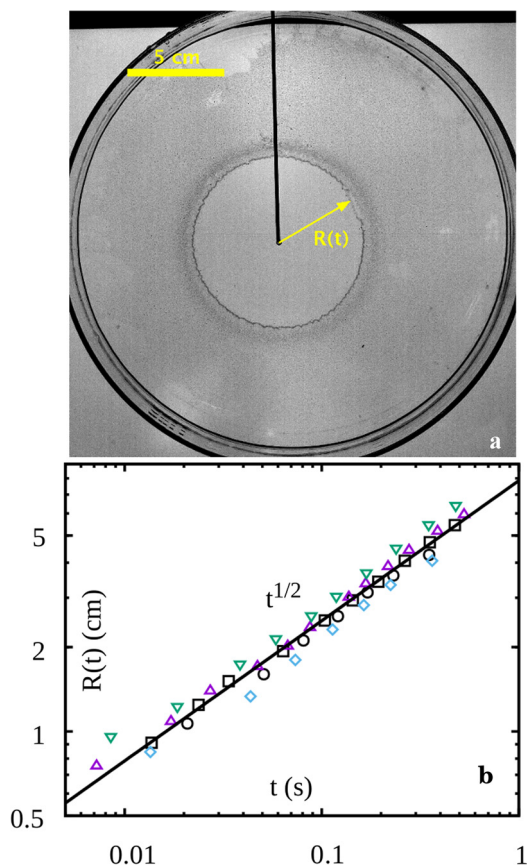


**Fig. 2.** (a) Visualization of camphoric acid spread radius. The water surface is uniformly covered with 50  $\mu\text{m}$  hollow glass spheres at low packing fractions to visualize the spread dynamics. Scale bar: 5 cm, (b) spread radius vs. time follows a  $t^{1/2}$  scaling law. Different symbols indicate different trials.

where there is no asymmetry in surface tension to drive the motion (hence *no* force on the boat) and/or (2) the drag force (by virtue of OA drop moving through the substrate fluid) starts opposing the boat motion. When the surface tension force equals the drag force the boat moves with terminal speed (mode 2). When the boat is exhibiting rectilinear motion, it is easy to show that the driving force or the surface tension force  $|\vec{F}|$  scales as  $\sim \Delta\sigma a$  where  $\Delta\sigma$  is the surface tension difference between the immediate “front” and “back” of the boat and  $a$  is the diameter of the boat. Note that, the “front” refers to the direction of motion and “back” refers to the opposite direction. As mentioned earlier, when there are symmetric surface tension gradients  $\Delta\sigma = 0$  however when in motion the c-boat experiences higher surface tension in the “front” compared to the “back” therefore  $\Delta\sigma > 0$ . Owing to continuous CA dissolution from the surface into the bulk fluid, the c-boat motion continues until it exhausts all CA molecules. Whereas dissolution does globally reduce the surface tension of water, a single boat contains ( $\sim 7 \times 10^{-6}$  kg) insufficient amount of CA to achieve an appreciable reduction in the ambient surface tension *via* dissolution; surface tension of CA saturated water is  $\sim 60 \times 10^{-3} \text{ N}\cdot\text{m}^{-1}$ .

Over the course of an experiment, water replaces CA removed from the boat starting at the tablet’s periphery and progressively proceeds radially inwards towards the tablet’s center (Fig. 4). Consequently, CA concentration at the c-boat edge constantly decreases resulting in low surface tension difference  $\Delta\sigma$  which causes reduction in boat speed as time progresses. In Fig. 3a, we show the mean c-boat speed (moving average over 1 minute interval) monotonically decreases with time. With decreasing driving force in time, the c-boat exhibits three distinct modes of motion. Figs. 3b–d show time traces of instantaneous c-boat speed

at specific intervals corresponding to these three modes. At early times the large driving force accelerates the c-boat to larger speeds however the drag force proportionately increases with speed and decelerates it. The acceleration and deceleration cycle leads to the harmonic oscillations about a mean speed (see Fig. 3b). This mean speed and oscillation frequency continuously decrease with time and transitions to the second distinct mode where the c-boat moves with steady or terminal speed (see Fig. 3c) as a result of equal driving and drag forces. The third distinct mode of intermittent motion emerges at long times and low surface tension differences where c-boat motion occurs intermittently (see Fig. 3d).

As the case with usual Marangoni force driven motion, the object of interest (*here* the c-boat) always moves to a location of high surface tension. The three essential steps in c-boat motion are 1. spreading of CA onto the water surface to create axially symmetric low surface tension region or the region of influence (ROI). 2. spontaneous symmetry breaking 3. escaping the region of low surface tension. In modes 1 and 2, while in motion, the asymmetry in surface tension gradients is maintained by the boat motion and hence no need for step 2. Whereas in mode 3 the boat motion completely stopped therefore the three steps need to start over and again. There exist two time scales  $\tau_1$  and  $\tau_3$  corresponding to steps 1 and 3 (Fig. 3d). Note that, there is *no* time scale associated with step 2 and it is worthwhile to mention that in mode 3 (Fig. 3d) the surges in speed are only approximately separated by  $\tau_1$  because of the stochastic nature associated with symmetry breaking. We identify  $\tau_1$  as the time required for the spread of CA onto water surface which has been discussed earlier. The second time scale  $\tau_3$  is the time required for the object to escape the ROI. The harmonic, steady and intermittent modes are observed when  $\tau_1 < \tau_3$ ,  $\tau_1 \sim \tau_3$  and  $\tau_1 > \tau_3$  respectively.

To reproduce and verify the role of surface tension on the existence of three modes of motion, we independently modified the ambient (far away from the influence of CA) surface tension using SDS at concentrations lower than Critical Micelle Concentration (CMC). When the c-boat experiment is conducted on SDS–water solutions, at the molecular level the water surface is populated with both SDS and CA molecules however SDS is a surfactant and is energetically more favorable for SDS to remain at the surface. Note that, CA is *not* a surfactant as it lacks the head and tail groups which are typically found in a surfactant. At intermediate concentrations of SDS, the ambient surface tension is modified solely by SDS whereas near the c-boat the reduction in surface tension is the combined effect of both SDS and CA. At higher concentrations, the surface is totally occupied by SDS and CA has *minor* role in modifying the surface tension. We speculate that any ambient surface modification is primarily dominated by SDS and secondary effects might be present due to the interaction between SDS and CA molecules. This speculation, though indirectly, is supported by the qualitative reproduction of the three modes. Furthermore, Nakata et al. [31,32] extensively studied the effect of different surfactants and the corresponding tail group chain lengths on the motion of camphor and camphoric acid tablets on water. The current observations are in accordance with their conclusions.

When the ambient surface tension ( $\gamma$ ) reduced to  $\gamma = 59 \times 10^{-3} \text{ N}\cdot\text{m}^{-1}$  the c-boat motion ceases as dissolution of CA has no further effect on water surface tension. The c-boat exhibited all the three modes of motion (Fig. 5) at surface tensions ranged between  $\gamma = 72 \times 10^{-3} \text{ N}\cdot\text{m}^{-1}$  and  $\gamma = 59 \times 10^{-3} \text{ N}\cdot\text{m}^{-1}$  in the *same order* as when no SDS was used. Note that this is *only* a qualitative reproduction of the effect. The exact values of surface tensions at those instants corresponding to Figs. 3b–d can not be measured as the c-boat is in motion. See S3.avi in the supplementary info for the motion of c-boat at  $\gamma = 65 \times 10^{-3} \text{ N}\cdot\text{m}^{-1}$ . Each mode was observed immediately few minutes after placing the c-boat on the water surface unlike the case when no SDS is used where each

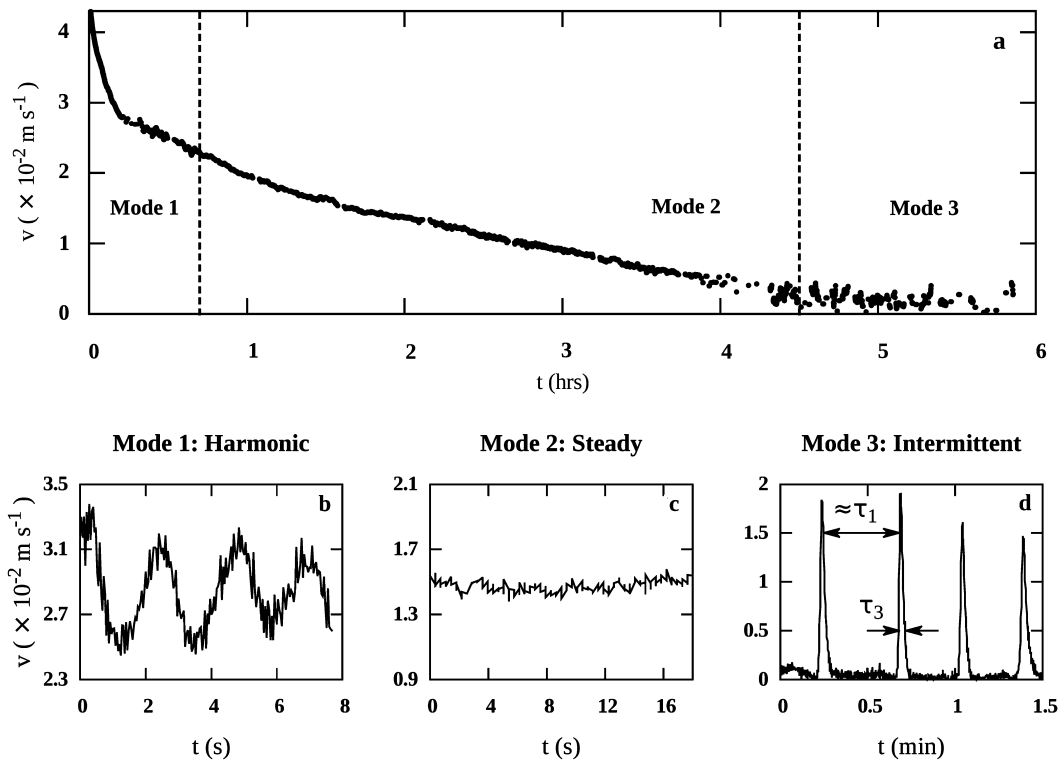


**Fig. 3.** (a) Monotonic decrease in mean c-boat speed (1 minute running average) over a 6 hour period, during which the c-boat exhibits three distinct modes of motion: (b) Harmonic mode with oscillating speed, (c) steady mode with constant speed, and (d) intermittent mode with long intervals of near-zero speed interspersed with sudden jumps.

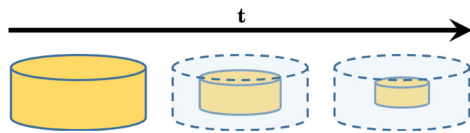


**Fig. 4.** Schematic of the structure of a c-boat as a function of time. As camphoric acid dissolves, water replaces camphoric acid in the gel matrix resulting in structural intactness of the c-boat. This process results in low CA (hence high surface tension) at the edge of the c-boat.

mode was discovered as the CA dissolved (Fig. 3). In conclusion, decreasing ambient surface tension using SDS and increase in surface tension at the edge of the c-boat due to dissolution of CA (Fig. 4) have the same effect on c-boat motion.

#### 4. Summary

In summary, we have studied the self-motion of a camphoric acid boat at the air–water interface and identified three distinct modes of motion. Each of the harmonic, steady-state, and intermittent modes have been separately reported [23–25,12] for objects

undergoing Marangoni propulsion. We have explained the existence of these propulsive modes as a consequence of CA concentration or Marangoni force strength, which we verified by controlling the surface tension of ambient interface through controlled doses of SDS. Furthermore, we identified the existence of two time scales  $\tau_1$  and  $\tau_3$  corresponding to CA spread and boat motion respectively and the disparity between  $\tau_1$  and  $\tau_3$  lead to the existence of the three modes. We anticipate these modes will contribute to the understanding of collective interactions between multiple c-boats within the context of active matter physics [17] as well as autonomous motion and self-assembly [20], the hydrodynamics of spreading of camphor acid and other volatile surfactants at air–water interfaces [30] as well as viscous Marangoni propulsion [18] among other studies.

#### Acknowledgements

VSA, DKS, and MMB were supported by the Collective Interactions Unit, OIST Graduate University. MMB acknowledges L. Mahadevan for introducing the camphor boat system and scientific discussions, and D. Vu Anh for help with preliminary experiments.

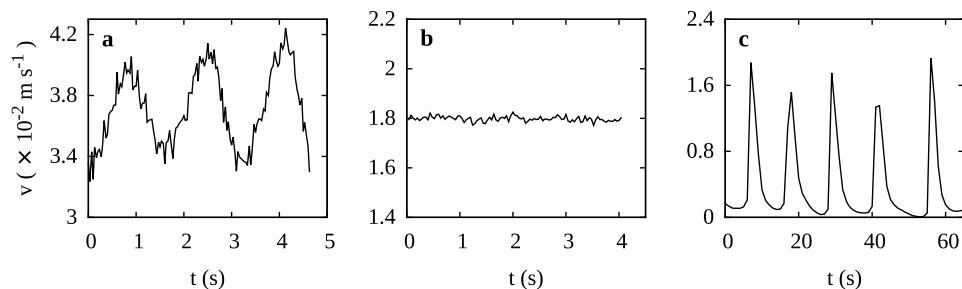


**Fig. 5.** Varying surface tension of water using SDS allows one to demonstrate all three c-boat propulsion modes: (a) Harmonic mode at  $\gamma = 72 \times 10^{-3} \text{ N} \cdot \text{m}^{-1}$ , (b) steady mode at  $\gamma = 68 \times 10^{-3} \text{ N} \cdot \text{m}^{-1}$ , and (c) intermittent mode at  $\gamma = 65 \times 10^{-3} \text{ N} \cdot \text{m}^{-1}$ .



The authors acknowledge Kenneth Meacham III for experimental support, Prof. Amy Shen for help with tensiometry measurements, and helpful discussions with Prof. Pinaki Chakraborty.

### Appendix A. Supplementary material

Supplementary material related to this article can be found online at <https://doi.org/10.1016/j.physleta.2018.02.026>.

### References

- [1] P. Neogi, Tears-of-wine and related phenomena, *J. Colloid Interface Sci.* 105 (1) (1985) 94–101.
- [2] R. Vuilleumier, V. Ego, L. Neltner, A.M. Cazabat, Tears of wine: the stationary state, *Langmuir* 11 (1995) 4117–4121.
- [3] K.C. Mills, B.J. Keene, R.F. Brooks, A. Shirali, Marangoni effects in welding, *Philos. Trans. R. Soc. Lond. A* 356 (1998) 911–925.
- [4] Heyde, *Centuria Observationum Medicarum*, 1686.
- [5] A. Volta, *Delectus Opusculorum Medicorum*, Ticini, 1787.
- [6] G.B. Venturi, *Ann. Chim. Phys.* 21 (1797) 262.
- [7] J.B. Biot, *Bull. Soc. Philomath. Paris* 54 (1801) 42–45.
- [8] L. Rayleigh, Measurements of the amount of oil necessary in order to check the motions of camphor upon water, *Proc. R. Soc. Lond.* 47 (1889) 364–367.
- [9] G.L. Van der Mensbrugge, Sur la tension superficielle des liquides considérée au point de vue de certains mouvements observés à leur surface, vol. 1, Hayez, 1869.
- [10] C. Tomlinson, On the motions of camphor on the surface of water, *Philos. Mag.* 38 (1869) 409–424.
- [11] M.K. Chaudhury, G.M. Whitesides, How to make water run uphill, *Science* 256 (1992) 1539–1541.
- [12] R. Sharma, S.T. Chang, O.D. Velev, Gel-based self-propelling particles get programmed to dance, *Langmuir* 28 (2012) 10128–10135.
- [13] S. Thutupalli, R. Seemann, S. Herminghaus, Swarming behavior of simple model squirmers, *New J. Phys.* 13 (2011).
- [14] M.I. Kohira, Y. Hayashima, M. Nagayama, S. Nakata, Synchronized self-motion of two camphor boats, *Langmuir* 17 (2001) 7124–7129.
- [15] F. Takabatake, N. Magome, M. Ichikawa, K. Yoshikawa, Spontaneous mode-selection in the self-propelled motion of a solid/liquid composite driven by interfacial instability, *J. Chem. Phys.* 134 (2011).
- [16] K.H. Nagai, K. Tachibana, Y. Tobe, M. Kazama, H. Kitahata, S. Omata, M. Nagayama, Mathematical model for self-propelled droplets driven by interfacial tension, *J. Chem. Phys.* 144 (2016).
- [17] S. Ramaswamy, The mechanics and statistics of active matter, *Annu. Rev. Condens. Matter Phys.* 1 (2010) 323–345.
- [18] E. Lauga, A.M.J. Davis, Viscous Marangoni propulsion, *J. Fluid Mech.* 705 (2012) 120–133.
- [19] S. Nakata, Y. Iguchi, M. Kuboyama, T. Ishii, K. Yoshikawa, Self-rotation of a camphor scraping on water: new insight into the old problem, *Langmuir* 13 (1997) 4454–4458.
- [20] R.F. Ismagilov, A.S. Schwartz, N. Bowden, G.M. Whitesides, Autonomous movement and self-assembly, *Angew. Chem., Int. Ed. Engl.* 41 (2002) 652–654.
- [21] R. Geryak, V.V. Tsukruk, Reconfigurable and actuating structures from soft materials, *Soft Matter* 10 (2014) 1246–1263.
- [22] L. Hu, B. Yuan, J. Liu, Liquid metal amoeba with spontaneous pseudopodia formation and motion capability, *Sci. Rep.* 7 (2017).
- [23] Y. Hayashima, M. Nagayama, S. Nakata, A camphor grain oscillates while breaking symmetry, *J. Phys. Chem. B* 105 (2001) 5353–5357.
- [24] N.J. Suematsu, Y. Ikura, M. Nagayama, H. Kitahata, N. Kawagishi, M. Murakami, S. Nakata, Mode-switching of the self-motion of a camphor boat depending on the diffusion distance of camphor molecules, *J. Phys. Chem. C* 114 (2010) 9876–9882.
- [25] H. Jin, A. Marmur, O. Ikkala, R.H.A. Ras, Vapour-driven Marangoni propulsion: continuous, prolonged and tunable motion, *Chem. Sci.* 3 (2012) 2526–2529.
- [26] Y. Hayashima, M. Nagayama, Y. Doi, S. Nakata, M. Kimurac, M. Iidac, Self-motion of a camphoric acid boat sensitive to the chemical environment, *Phys. Chem. Chem. Phys.* 4 (2002) 1386–1392.
- [27] H. Kitahata, S. ichi Hiromatsu, Y. Doi, S. Nakata, M.R. Islam, Self-motion of a camphor disk coupled with convection, *Phys. Chem. Chem. Phys.* 6 (2004) 2409–2414.
- [28] S. Soh, K.J.M. Bishop, B.A. Grzybowski, Dynamic self-assembly in ensembles of camphor boats, *J. Phys. Chem.* 112 (2008) 10848–10853.
- [29] K.J. Mysels, Surface tension of solutions of pure sodium dodecyl sulfate, *Langmuir* 2 (1986) 423–428.
- [30] A.D. Dussaud, S.M. Troian, Dynamics of spontaneous spreading with evaporation on a deep fluid layer, *Phys. Fluids* 10 (1998) 23–38.
- [31] S. Nakata, J. Kirisaka, Y. Arima, T. Ishii, Self-motion of a camphoric acid disk on water with different types of surfactants, *J. Phys. Chem. B* 110 (2006) 21131–21134.
- [32] S. Nakata, M. Murakami, Self-motion of a camphor disk on an aqueous phase depending on the alkyl chain length of sulfate surfactant, *Langmuir* 26 (4) (2010) 2414–2417.